Program Digest, 2019 IEEE International Ultrasonics Symposium (IUS)
Glasgow, Scotland, October 6-9, 2019

High Frequency Piezoelectric Micromachined Transducers with Wide Bandwidth and High Sensitivity

Corina Nistorica
FUJIFILM Dimatix, Inc.
Santa Clara, USA
cnistorica@fujifilm.com

Dimitre Latev
FUJIFILM Dimatix, Inc.
Santa Clra, USA
dlatev@fujifilm.com

Takahiro Sano
FUJIFILM Corporation
Kaisei, Japan
takahiro.a.sano@fujifilm.com

Liuyi Xu
FUJIFILM Dimatix, Inc.
Santa Clara, USA
sxu@fujifilm.com

Darren Imai
FUJIFILM Dimatix, Inc.
Santa Clara, USA
dimai@fujifilm.com

***Abstract*—Recent advances in microfabrication and piezoelectric thin film deposition have made possible the fabrication of micromachined ultrasound transducers that can compete in performance with the traditional bulk piezoelectric transducers. In this paper we report a piezoelectric micromachined transducer (PMUT) with 128 elements, a center frequency of 12MHz, a bandwidth of 105% and a sensitivity of -56dB at 15 mm from transducer. Design, characterization, matching circuit and ultrasound images acquired with the PMUT device are described in this work.**

Keywords—PMUT, MEMS, PNZT, piezoelectric, ultrasound

I. INTRODUCTION

The healthcare market is the newest driver of opportunities in the MEMS industry with health mobility being one of the emerging applications. Piezoelectric micromachined transducers (PMUT) represent a novel approach for the construction of miniaturized, low-power portable ultrasound systems and catheter transducer arrays. Piezoelectric Micromachined Transducers are well suited for medical applications such as general ultrasound imaging probes, catheters and sensors that require high volume manufacturing, low cost as well as high levels of integration and miniaturization. Compared to the better known capacitive micromachined transducers [1], PMUT transducers have the advantage that they do not require high voltage bias, are easier to fabricate, have better long-term reliability and lower electrical impedance providing a better match to the ultrasound system readout electronic. Although low frequency PMUT transducers have been reported in literature [2], they usually had very limited bandwidth and sensitivity. The present study describes the design, fabrication and characterization of a high frequency (12 MHz) PMUT transducer with large bandwidth and high sensitivity. The frequency range and overall dimensions of this PMUT transducer could be useful for musculoskeletal examinations, vascular access or nerve blocks imaging at a depth of 4cm in the acoustic medium.

II. DESIGN

A. Materials and Structure

The material used in the fabrication of PMUT transducers at FUJIFILM Dimatix was a proprietary RF-sputtered, high performance and reliable niobium-doped lead zirconate titanate (PNZT) film with a very high piezoelectric coefficient $e_{31,f}$=-20C/m^2 [3]. The PNZT film is prepoled in the as-grown state, making a poling process unnecessary. Post processing of the PNZT film can be done at temperatures as high as 400ºC without any deterioration of the piezoelectric properties. The transducer analyzed in this paper is a 128 element linear array. The transducer had a backing layer made out of tungsten microspheres embedded in an epoxy. The transducer was developed to be used in an ultraportable ultrasound system, the design targeting wide bandwidth and high sensitivity. Although our group has previously reported dome shaped membrane PMUT arrays [4], a flat PMUT membrane structure was used in this work. The flat PMUT membrane ensures a very simple fabrication process and very high yield. Each element was composed of multiple circular membranes having a wide range of radii while their thickness was defined by the piezoelectric film thickness plus the silicon oxide membrane thickness. A wide bandwidth design has been achieved by overlapping the frequency response of multiple circular resonators having various diameters and various resonant frequencies. Larger PMUT cells were positioned in the center of the element, with the diameter of the cell gradually decreasing towards the ends of the element as shown in Fig.1. This arrangement of the PMUT cells provides a beam shape that is very similar to the beam shape of a traditional piston type piezoelectric transducer. The circular PMUT cells were positioned in a hexagonal arrangement to achieve highest possible fill factor for a certain pitch and elevation of the transducer element. The

fill factor is defined as the ratio of the active area of the moving membranes of the resonator cells and the total area of the element. With the distance between the circular cells being as small as 5 µm, a fill factor of 70% was achieved warranting a high sensitivity for the device.

Finite element modeling (FEM) of the PMUT array has been performed using commercially available simulation software, the models being used to guide the design optimization of such complex multifrequency arrays. The diameter of the top electrode and the PNZT as well as the thickness of every layer has been optimized using the FEM simulation and following the required fabrication rules.

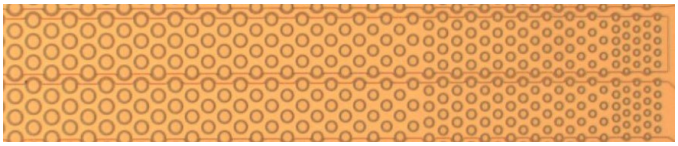

Fig. 1. Optical image of PMUT cell arrangement in an element. A section of the transducer element shown in picture.

The main design characteristics of the transducer chosen for this study are presented in TABLE I.

TABLE I. TRANSDUCER DEFINITION

Device	Multi-frequency
Aperture	20 mm
Elevation	2.75 mm
Pitch	156 µm
Elements	128
Membrane radius	13 µm -23 µm

B. Matching Circuit

In order to maximize the PMUT performance, an electric impedance matching circuit is required [5-7]. The electric impedance matching network (EIMN) presented in this work was designed for increased bandwidth of pulse-echo impulse response. Many other designs are possible for the matching circuit, some of them targeting increased bandwidth others increased sensitivity or a combination of the two. The electric impedance of a single PMUT element was measured by an Agilent E5061B ENA Series Network Analyzer. The electric mismatch losses were calculated from the electric impedance difference between the transducer and the driving amplifier output impedance of 50 Ω.

The EIMN was designed as a LC ladder filter structure. The acoustic characteristics of the PMUT with the EIMN were measured by inserting the EIMN between transmission BNC cable and the transducer.

III. RESULTS

The transducer's performance was assessed from measurements of the pulse-echo impulse response, transmit sensitivity, pulse-echo sensitivity, electrical impedance, far field pressure level, and the acoustic beam directivity.

The transducer was packaged with a flex circuit and low profile connector, backing material and a thin silicone rubber front lens.

A. Pulse-Echo Sensitivity and Bandwidth

The mismatch loss was initially measured without a matching circuit added to the transducer circuit. The EIMN was designed and applied to the PMUT array. The mismatch loss frequency dependence for one array element is shown in Fig. 2. From the solid line in Fig. 2, it was found that the PMUT has more than 3 dB of mismatch loss in one way of pulse-echo scheme. Thus, there is a 6 dB loss in the pulse-echo sensitivity in wide frequency range due to mismatch loss. In order to increase the bandwidth, the mismatch loss was modified as shown by the dotted line in Fig. 2 by using the matching circuit shown in the inset in Fig 2. The EIMN decreases the mismatch loss at both frequency edges where the pulse-echo sensitivity was initially measured to be -6 dB lower than peak sensitivity. The EIMN was composed of 2 capacitors and 2 inductors. The component values were L_1 = 220 nH, C_1 = 220 pF, C_2 = 3.3 nF, and L_2 = 470 nH. Although the matching circuit presented in this work had a total of 4 components, other combinations, with fewer components are possible.

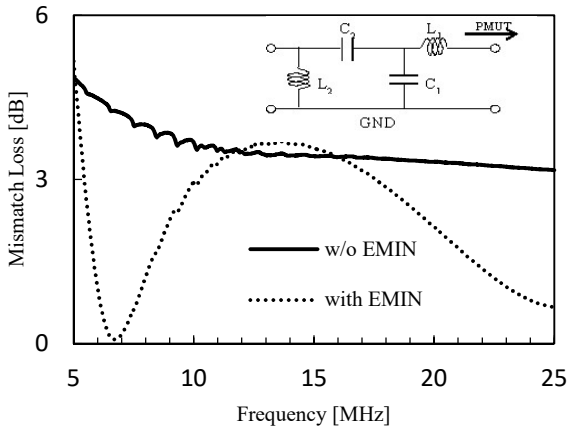

Fig. 2. Electric impedance mismatch loss between PMUT element and the 50 ohm line.

The results of the pulse-echo measurement performed with the EIMN added to the transducer, are presented in Fig. 3. The pulse-echo sensitivity measurement was performed in a dedicated water tank setup named Acoustic Intensity Measurement System (AIMS) from ONDA Corporation and using a stainless steel plate reflector. The pulse-echo waveform and echo frequency spectrum show a fractional bandwidth of 105% at -6dB, confirming an increase of 23% of the bandwidth compared to the case without a matching circuit. The increase in bandwidth was achieved without any sensitivity drop. The pulse length, measured between the first and last point in the pulse waveform at -20dB to the amplitude peak, is 250 ns, suggesting good image resolution can be achieved with this transducer.

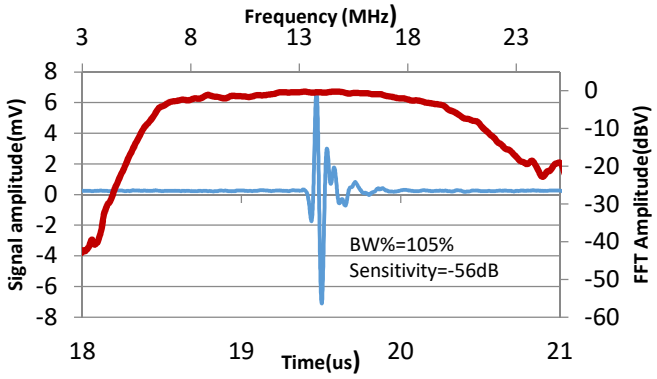

Fig. 3. Pulse-echo impulse response and its Fourier transform as measured in water for an element of the PMUT transducer. Driving Voltage was a 10V pulse.

The pulse-echo response and sensitivity were characterized at ever increasing depths in the water tank by placing the stainless steel plate reflector at ever increasing distance from the transducer. The pulse-echo sensitivity measured versus depth in the water tank is presented in Fig. 4. The loop sensitivity is -54dB at 5mm distance from transducer and decreases to -70dB at 40 mm distance from transducer in water. These values ensure that quality ultrasound images can be acquired at these depths of interest.

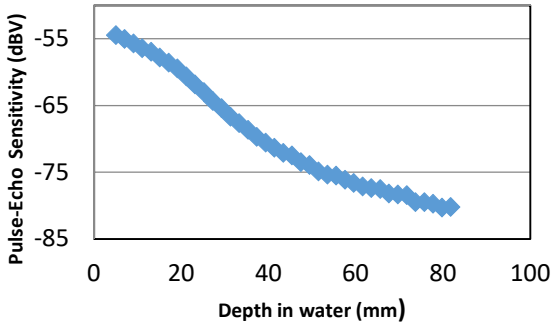

Fig. 4. Pulse Echo Sensitivity of the PMUT transducer measured in water with a flat stainless steel reflector placed at a certain depth from transducer.

The PMUT element transmit acoustic pressure sensitivity measurements, shown in Fig. 5, were performed using a calibrated hydrophone (ONDA HGL-0085) and a dedicated water tank setup AIMS. We characterized the electroacoustic transmit response with the hydrophone being placed at ever increasing depth in the water tank. The transducer was excited by a 25 ns pulse. High transmit sensitivity of 12kPa/V was achieved at 1 mm from the surface of the transducer and 4kPa/V at 40mm depth in water. A good match was found between the measured values and the FEM simulation.

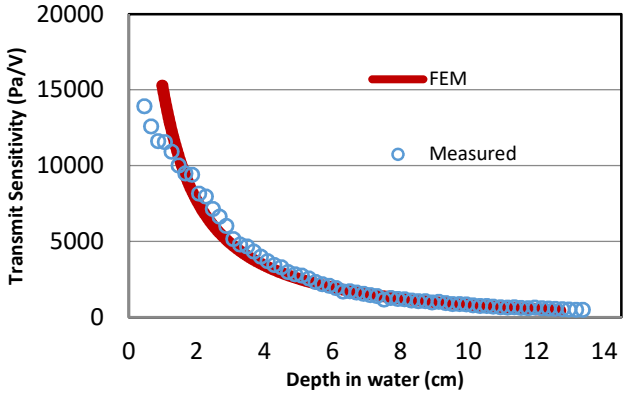

Fig. 5. Transmit pressure sensitivity versus depth in water: simulation versus measurement.

In order to characterize the directivity of the transducer, acoustic field measurements were performed by scanning the hydrophone in both azimuth direction and elevation direction. Fig. 7 illustrates the beam patterns determined from the measured peak-to-peak voltage of the hydrophone normalized to the maximum value. The beam pattern has a similar shape to a traditional piston-like bulk piezoelectric transducer, confirming the advantageous arrangement of the PMUT cells for this particular design.

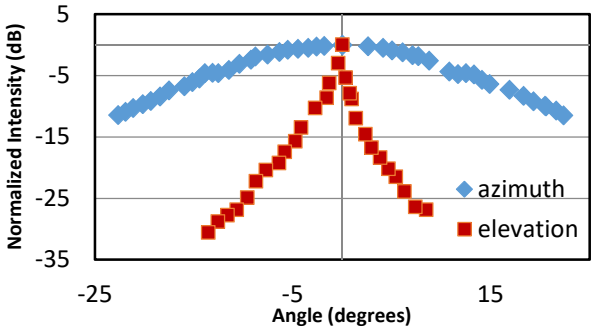

Fig. 6. Acoustic beam shape in azimuth and elevation direction..

B. *Electrical Impedance*

Electrical impedance was first measured for a transducer without a front silicone lens in air. Multiple resonances are present in this case corresponding to the resonant frequencies of the PMUT membranes with various diameters as shown in Fig. 7. Other than the main resonance of each cell membrane, additional resonances can be observed in the impedance measurement. These resonances are the result of interaction between the different resonators composing one single element. When a silicone lens is molded on the surface of the transducer, the vibrating membranes are mechanically loaded and the quality factor of each individual resonating membrane is decreasing. This allows multiple resonances to merge, the result being a wide bandwidth transducer. This also indicates good coupling between the resonator membranes and the acoustic medium. The impedance of the transducer at the frequency of interest is 14 ohm.

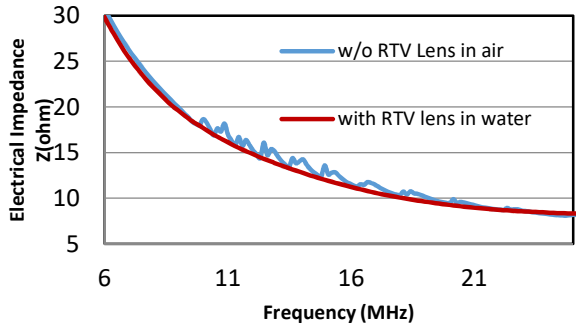

Fig. 7. Electrical Impedance measured in air without a front RTV lens and in water with a front silicone lens.

C. *Ultrasound Imaging*

Images of a wire ultrasound phantom have been acquired using a Verasonics imaging system. The ultrasound phantom images revealed good penetration depth of more than 4 cm and good resolution as shown in Fig. 8. Images were acquired with the PMUT transducer actuated at a low voltage of 20V demonstrating good transducer sensitivity. The transducer is able to image 80 µm diameter wires with a separation of 250 µm axially and a separation of 500 µm laterally.

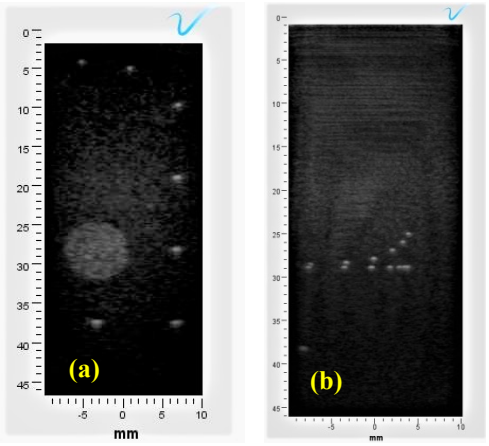

Fig. 8. Images of the CIRS 040GSE Ultrasound Phantom acquired with the PMUT transducer operating at 20V. Ultrasound Phantom wires are 100 µm in diameter for image (a) on the left and 80 µm in diameter for image (b)on the right.

The Ultrasound images were acquired up to 45 mm depth using a plane wave type of imaging algorithm. The images represent raw data, without any image post processing.

The overall performance of PMUT arrays in terms of center frequency, bandwidth and sensitivity, is greatly dependent not only on the design of each resonator cell composing an element, but also on the arrangement of the cells within the element.

IV. CONCLUSIONS

This paper has described the design, fabrication and characterization of a 12 MHz PMUT array with very wide bandwidth and high sensitivity. Such high sensitivity, low operating voltage and ease of fabrication makes the PMUT array a good solution for ultraportable ultrasound imaging probes. Also, adding the potential for miniaturization and integration with supporting electronics, the PMUT arrays are ideal for catheter based applications. The PMUT arrays show great potential for real-time 3D imaging using complex 2D PMUT arrays with large number of elements, and high-frequency applications such as intra-vascular imaging.

REFERENCES

[1] A. S. Savoia, G. Caliano, M. PAppalardo, “A CMUT Probe for Medical Ultrasonography: From Microfabrication to System Integration”, IEEE Trans. Ultrason. Ferroelect. Freq. Control, vol. 59.,pp1127- 1137, 2012.

[2] D.E. Dausch, J.B. Castelucci, D.R. Chou, O.T. von Ramm, “Theory and Operation of 2-D Array piezoelectric Micromachined Transducers” IEEE Trans. Ultrason., Ferroelect., Freq. Contr., vol.55, pp 2484-2492, 2008.

[3] Y. Hishinuma, Y. Li, J. Birkmeyer, T. Fujii, T. Naono, and T. Arakawa, “High Performance Sputtered PZT Film for MEMS applications” Nanotech 2, 137-140 ,2012.

[4] C.Nistorica, D.Latev, J. Mendoza, D.Imai, “Modeling and Characterization of a 3D-MEMS Piezoelectric Ultrasound Transducer”, IEEE International Ultrasonics Symposium, 2016.

[5] Molchanov V. Y. and Makarov O., “Phenomenological method for broadband electrical matching of acousto-optical device piezotransducers,” Opt. Eng., 38, 1127–1135,1999.

[6] San Emeterio J. L., Ramos A., Sanz P. T., and Ruiz A., “Evaluation of impedance matching schemes for pulse-echo ultrasonic piezoelectric transducers,” Ferroelectrics, 273, 297–302,2002.

[7] Garcia-Rodriguez M., Garcia-Alvarez J., Yañez, Y., Garcia-Hernandez M. J., Salazar J., Turo A., and Chavez J. A., “Low cost matching network for ultrasonic transducers,” Phys. Procedia, 3, 1025–1031,2010.

[8] Kim M. G. Yoon S., Kim H. H., and Shung K. K., “Impedance matching network for high frequency ultrasonic transducer for cellular applications,” Ultrasonics, 65, 258–267, 2016.

[9] Moon J. Y., Lee, J., and Chang J. H., “Electrical impedance matching networks based on filter structures for high frequency ultrasound transducers,” Sens. Actuators A, 251, 225–233, 2016.